

1 **Genetic mechanisms of primary chemotherapy resistance in pediatric acute myeloid leukemia: A
2 report from the TARGET initiative**

3
4 ***Running Title: Genomics of induction failure in pediatric acute myeloid leukemia***
5 Nicole A. McNeer¹⁺, John Philip¹⁺, Heather Geiger⁴, Rhonda E. Ries², Vincent-Philippe Lavallée³, Michael
6 Walsh¹, Minita Shah⁴, Kanika Arora⁴, Anne-Katrin Emde⁴, Nicolas Robine⁴, Todd A Alonzo⁵, E. Anders
7 Kolb⁶, Alan S Gamis⁷, Malcolm Smith⁸, Daniela Se Gerhard⁸, Jaime Guidry-Auvil⁸, Soheil Meshinchi^{2*}, Alex
8 Kentsis^{1,9,10*}

9
10 ¹Department of Pediatrics, Memorial Sloan Kettering Cancer Center, New York, NY
11 ²Fred Hutchinson Cancer Research Center, Seattle, WA
12 ³Computational and Systems Biology Program, Sloan Kettering Institute, Memorial Sloan Kettering
13 Cancer Center, New York, NY

14 ⁴New York Genome Center, New York, NY
15 ⁵Department of Biostatistics, University of Southern California, Los Angeles , CA
16 ⁶Nemours Center for Cancer and Blood Disorders, Nemours/Alfred Dupont Hospital for Children,
17 Wilmington, DE
18 ⁷University of Missouri-Kansas City School of Medicine, Kansas City, MO
19 ⁸National Cancer Institute, Rockville, MD
20 ⁹Molecular Pharmacology Program, Sloan Kettering Institute, Memorial Sloan Kettering Cancer Center,
21 New York, NY
22 ¹⁰Department of Pediatrics, Pharmacology, and Physiology & Biophysics, Weill Medical College of
23 Cornell University, New York, NY

24
25 ⁺ Equal contribution
26
27 * Correspondence to A.K. (kentsisresearchgroup@gmail.com) and S.M. (smeshinc@fhcrc.org)
28

29 **Conflicts of Interest.** A.K. is a consultant for Novartis.

30

31 **Abstract**

32

33 Acute myeloid leukemias (AML) are characterized by mutations of tumor suppressor and oncogenes,
34 involving distinct genes in adults and children. While certain mutations have been associated with the
35 increased risk of AML relapse, the genomic landscape of primary chemotherapy resistant AML is not
36 well defined. As part of the TARGET initiative, we performed whole-genome DNA and transcriptome
37 (RNA and miRNA) sequencing analysis of pediatric AML with failure of induction chemotherapy. We
38 identified at least three genetic groups of patients with induction failure, including those with *NUP98*
39 rearrangements, somatic mutations of *WT1* in the absence of *NUP98* mutations, and additional
40 recurrent variants including those in *KMT2C* and *MLLT10*. Comparison of specimens before and after
41 chemotherapy revealed distinct and invariant gene expression programs. While exhibiting overt therapy
42 resistance, these leukemias nonetheless showed diverse forms of clonal evolution upon chemotherapy
43 exposure. This included selection for mutant alleles of *FRMD8*, *DHX32*, *PIK3R1*, *SHANK3*, *MKLN1*, as well
44 as persistence of *WT1* and *TP53* mutant clones, and elimination or contraction of *FLT3*, *PTPN11*, and
45 *NRAS* mutant clones. These findings delineate genetic mechanisms of primary chemotherapy resistance
46 in pediatric AML, which should inform improved approaches for its diagnosis and therapy.

47

48

49 **Introduction**

50

51 Overall survival for children with acute myeloid leukemia (AML) remains low, due principally to
52 the failure to achieve durable disease remission after initial induction therapy. Failure rate of primary
53 induction remission therapy in pediatric AML is 10-15%, and only about a third of patients for whom
54 primary induction therapy fails are ultimately cured (1). Reasons for the lack of response to initial
55 chemotherapy in pediatric AML remain unclear, and a molecular understanding of this process is
56 needed.

57 Since the first AML genome was sequenced (2, 3), numerous genomic profiling studies have
58 revealed diverse disease subtypes and distinct genetic modes of disease relapse (4). For example,
59 whole-genome sequencing of AML specimens from adults with relapsed disease revealed broad
60 patterns of clonal evolution, suggesting that either founding clones gained mutations upon relapse, or
61 that diagnostic subclones persisted with acquisition of additional mutations after therapy (5). Analysis of
62 whole exome capture sequencing from matched diagnosis, remission, and relapse trios from twenty
63 pediatric AML cases showed that responses of specific genetic clones were associated with disease
64 relapse (6). Similarly, clonal persistence after induction chemotherapy was found to be associated with
65 disease relapse in adult AML (7).

66 Recent study of primary chemotherapy resistance in a cohort of 107 children and adults with
67 AML using targeted gene sequencing demonstrated that few patients exhibited specific individual
68 mutations associated with primary chemotherapy resistance and failure of induction chemotherapy (8).
69 In addition, at least for some patients, chemotherapy resistance is caused by the epigenetic activation of
70 the transcription factor MEF2C (9-10). This suggests that there are additional genetic or molecular
71 mechanisms mediating primary chemotherapy resistance in pediatric and adult AML. Importantly,
72 pediatric AML is characterized by distinct genetic mutations and genomic rearrangements, with relative

73 paucity of the recurrent mutations frequently observed in adult AML (11). Thus, direct study of primary
74 chemotherapy resistance in pediatric AML is needed.

75 Here, we assembled a cohort of pediatric patients with primary chemotherapy resistance and
76 failure of induction chemotherapy, as part of the TARGET AML initiative. We analyzed whole-genome
77 DNA, mRNA, and miRNA sequence data, obtained at diagnosis and upon chemotherapy administration.
78 These studies revealed distinct classes of genetic mutations and their clonal evolution in chemotherapy
79 resistant disease, which should inform future approaches for the diagnosis, risk stratification and
80 therapeutic interventions for pediatric AML.

81

82 **Methods**

83

84 Complete methodological details are provided in the Supplementary Methods. All specimens
85 and clinical data were obtained from patients enrolled on biology studies and clinical trials managed
86 through the Children's Oncology Group (COG protocols AAML0531 and AAML03P1). Patient samples
87 were sequentially identified, and selected for comprehensive genomic profiling, if adequate amounts of
88 high-quality nucleic acids was available. Patient samples were collected as matched trios: bone marrow
89 aspirates pre-and post-treatment, and matched marrow fibroblasts. Details of sample preparation
90 protocols and clinical annotations and all primary data are available through the TARGET Data Matrix
91 (<https://ocg.cancer.gov/programs/target/data-matrix>). Whole-genome paired-end sequencing libraries
92 were prepared using the genomic 350-450bp insert Illumina library construction protocol with Biomek
93 FX robot (Beckman-Coulter, USA), sequenced with an average coverage of 30-fold using Illumina
94 HiSeq2500. Sequence files were mapped to the GRCh37 (hg19) genome, and processed to identify single
95 nucleotide variants (SNVs), insertions/deletions (indels), gene fusions, and structural variants. For
96 mRNA-sequencing, extracted RNAs was used to generate cDNAs using the SMART cDNA synthesis

97 protocol with the SMARTScribe reverse transcriptase (Clontech) and resultant libraries were sequenced
98 with 75 bp paired reads using Illumina HiSeq2500. RNA-seq reads were aligned with STAR (version
99 2.4.2a), and genes annotated in Gencode v18 were quantified with featureCounts (v1.4.3-p1). Fusion
100 genes were detected using FusionCatcher and STAR-Fusion. Resultant variant call files (VCFs) were
101 subsequently aggregated using an integrated script, available from
102 <https://github.com/kentsisresearchgroup/TargetInductionFailure>. VCFs were parsed to assemble single
103 nucleotide variants, indels, copy number variation, structural variants, and gene fusions in a master
104 table, and filtered to identify high-confidence calls. Normalization and differential expression was done
105 with the Bioconductor package DESeq2. Gene set enrichment analysis was performed using GSEA v2.2.1
106 plus MSigDB v6.0. All raw sequencing data are available via dbGaP accession numbers phs000465,
107 phs000178 and phs000218, with the processed mutational and expression data published via Zenodo
108 (<http://doi.org/10.5281/zenodo.1403737>).

109

110 **Results**

111

112 ***Genomic landscape of pediatric induction failure AML.*** A total of 28 patients with primary
113 chemotherapy resistance and failure of induction chemotherapy were studied. The patients were
114 uniformly treated as part of the COG AAML0531 study, having received cytarabine, daunorubicin and
115 etoposide (ADE10+3) chemotherapy. Demographic features of the study cohort are listed in
116 Supplemental Table 1, and are representative of the entire patient cohort, enrolled as part of the
117 AAML0531 study (12). True failure of induction chemotherapy was defined as morphologic persistence
118 of at least 5% of AML bone marrow blasts 28 or more days after therapy initiation, but prior to the
119 second course of induction chemotherapy (12). We used genomic DNA from cultured fibroblasts
120 isolated from the bone marrow as non-tumor germline DNA to identify somatically acquired mutations.

121 Using supervised analysis based on genes currently known to have cancer predisposition potential, we
122 did not identify any apparent pathogenic germline variants in this cohort (Supplemental Table 2). For
123 whole-genome DNA sequencing, we obtained mean coverage of 39 (range 23-69). mRNA and miRNA
124 sequencing data had on average 59% and 19% mapping coverage, respectively.

125 In agreement with prior studies (11), we found that this cohort of pediatric AML with induction
126 failure had fewer of the mutations commonly observed in adult AML, including *DNMT3A*, *TET2*, *IDH1/2*
127 and others (13). The most commonly called alterations observed in our cohort were rearrangements of
128 *NUP98*, and variants in *WT1*, *RUNX1*, *MLLT10*, *SPECC1*, and *KMT2C*, predominantly as a result of
129 genomic rearrangements and somatic structural variants (Figure 1A). In particular, we identified *NUP98-*
130 *NSD1* fusions, as well as a number of additional genomic rearrangements, leading to the production of
131 chimeric fusion genes, as evidenced by the combined genomic rearrangements in DNA, and the
132 presence of mRNA sequencing reads in RNA-seq data (Figure 1B). While mutations of *FLT3* and *KMT2C*,
133 and t(8;21), inv(16) and trisomy 8 alterations were the five most common events in the analysis of an
134 unselected cohort of pediatric AML patients (11), these abnormalities were substantially depleted in our
135 induction failure cohort. The relative and unselected enrichment for *NUP98-NSD1* rearrangements and
136 *WT1* mutations in this induction failure cohort is consistent with the reported poor prognosis of these
137 alterations, with a reported 4-year event-free survival of less than 10% (14).

138

139 ***Three genetic subtypes of pediatric AML with primary chemotherapy resistance.*** Although
140 diverse mutations were observed in our cohort, unsupervised hierarchical clustering was unable to
141 segregate the observed cohort into distinct classes. Therefore, we divided the patients into three groups
142 based on the most common recurrent mutations (Figure 2A). Group 1 (6 patients) was defined by the
143 presence of *NUP98* rearrangements, and additional mutations including *WT1*, *ELF1*, and *FRMD8*. No
144 specimens exhibited chromosomal monosomies or complex karyotypes. Although *FLT3* mutations are

145 often observed in *NUP98-NSD1* leukemias, group 1 did not appear to have *FLT3* mutations. The
146 association of *NUP98* rearrangements with *WT1* mutations in AML induction failure may be due to the
147 functional interaction between these two factors, since patients with both alterations are known to
148 have a much worse prognosis than either alone (11, 14, 15). In addition, we observed an association of
149 *NUP98* rearrangements with deletions of the ETS transcription factor *ELF1* and copy number gain of the
150 gene encoding cell adhesion signaling factor *FRMD8*, both of which have also been observed in myeloid
151 malignancies (16, 17). This association may involve similar cooperating interactions that presumably
152 cause intrinsic chemotherapy resistance. We also identified gain of *MYC* in two patients from group 1, in
153 agreement with prior finding of activating *MYC* mutations in association with *NUP98-NSD1* AML (18).

154 Group 2 (11 patients) was defined by the presence of *WT1* mutations without apparent *NUP98*
155 rearrangements, and also involves additional mutations including tyrosine kinase domain (TKD, SNV) and
156 internal tandem duplication (ITD, indel) in *FLT3*, and various other copy number changes and genomic
157 rearrangements. We observed both missense and nonsense *WT1* mutations, consistent with previous
158 reports in AML (19, 20, 21). In addition, group 2 included cases with copy number alterations involving
159 the *BCL11B*, *AKT1*, and *ARID1B* loci, among others (Figure 2A), as well as one patient specimen PATISD
160 with monosomy 7 (Supplemental Table 1). *BCL11B* is a known tumor suppressor gene mutated in
161 refractory forms of T-cell acute lymphoblastic leukemias (T-ALL) (19), including a subtype that may share
162 common origins with refractory AML (20). In addition, both *BCL11B* and *ARID1B* are components of the
163 SWI/SNF/BAF chromatin remodeling complex that is disrupted in diverse human cancers (22).

164 Group 3 (11 patients) was defined by the apparent absence of *NUP98* rearrangements and *WT1*
165 mutations, and instead includes leukemias with mutations of *KMT2C* and *MLLT10* (Figure 2A). *KMT2C* is
166 the tumor suppressor gene that encodes the MLL3 chromatin remodeling factor, that is also inactivated
167 in myeloid malignancies as a result of losses of chromosome 7q (23). Similarly, *MLLT10* is frequently
168 rearranged as part of *KMT2A/MLL1* and other chromosomal translocations in acute leukemias, including

169 refractory forms of T-ALL in particular (24) (25). Given the involvement of additional genes and loci
170 recurrently mutated or rearranged in this cohort of patients, it is probable that additional subtypes of
171 chemotherapy resistant disease exist.

172 Intriguingly, while only one patient in group 1 remained alive at 6 years after therapy, and three
173 patients remained alive in group 2, five survivors were observed in group 3. Though the size of this
174 cohort is not powered sufficiently to detect statistically significant differences in survival (log-rank $p =$
175 0.39, 0.70, and 0.55 for group 1 vs 2, 1 vs 3, and 2 vs 3 respectively), these results suggest that the
176 apparent diversity of genetic subtypes of induction failure may also be associated with variable clinical
177 outcomes.

178 Using mRNA sequencing, we analyzed gene expression programs associated with the primary
179 chemotherapy resistant AML, as assessed using gene set enrichment analysis in diagnostic samples
180 (Figure 2B). Unsupervised hierarchical clustering of gene expression profiles did not segregate with the
181 genetically defined groups (Supplemental Figure 1). This suggests that diverse genetic subtypes of
182 induction failure AML may engage common gene expression programs. This notion is consistent with the
183 recent study implicating epigenetic signaling by the transcription factor MEF2C in AML chemotherapy
184 resistance (9).

185 Lastly, we surveyed microRNA expression in diagnostic samples from this cohort, with the most
186 highly expressed miRNAs listed in Supplemental Table 3. We observed that miR-21 was highly expressed
187 among all 3 subgroups of induction failure patients, consistent with its reported association with inferior
188 clinical outcomes (26). Similarly, we observed high levels of expression of miR-10a, particularly in group
189 1. miR-10a upregulation has been reported in *NPM1*-mutant AML with associated MDM4
190 downregulation, potentially interfering with TP53 signaling (27). We also found high expression of miR-
191 103 in group 1 patients, which has been reported to downregulate *RAD51*, leading to dysregulated DNA
192 damage response (28). In addition, we found upregulation of miR-181a in groups 2 and 3, which has

193 been reported to be overexpressed and mediate ATM downregulation in AML cell lines (29). In all, these
194 findings are consistent with the proposed mechanisms of regulation of chemotherapy response by
195 miRNAs in AML (30).

196

197 **Diverse models of clonal evolution by induction chemotherapy.** We reasoned that exposure to
198 chemotherapy would lead to selection of genetic clones with mutations conferring chemotherapy
199 resistance, and contraction of clones that are susceptible to ADE chemotherapy. Thus, we compared the
200 prevalence of mutations among different patients in specimens collected before and after induction
201 chemotherapy (Figure 3). We found numerous genomic rearrangements and mutations that were
202 significantly increased in prevalence upon induction chemotherapy exposure. For example, we observed
203 that gains of the *FRMD8* locus were present in 7 of 28 (25%) patients at diagnosis, as compared to 20 of
204 28 (71%) patients post-chemotherapy (two-tailed Fisher's exact test $p = 1.1e-3$). This suggests that
205 genomic rearrangement involving *FRMD8* or linked genes may contribute to chemotherapy resistance.
206 *FRMD8* encodes a plasma membrane-associated FERM domain that can contribute to Wnt signaling and
207 processing of transmembrane precursors of inflammatory cytokines (31, 32). In addition, increased
208 *FRMD8* gene expression was found to be a marker of poor prognosis in adult AML (33).

209 Mutations and rearrangements of various additional genes with functions in cell adhesion and
210 signaling, including *FANK1*, *PIK3R1*, *SHANK3*, and *MKLN1*, also appear to be selected upon
211 chemotherapy exposure, suggesting that they may also contribute to therapy resistance. In contrast,
212 mutations of *FLT3* exhibited significant depletion upon chemotherapy administration (Figure 3A).
213 Aberrant activation of *FLT3* kinase signaling is a known oncogenic event in AML pathogenesis,
214 contributing to the enhanced proliferation and survival of AML cells, and is associated with inferior
215 prognosis when present at sufficiently high allelic frequencies (34-38). Its relative depletion by
216 chemotherapy in AML induction failure suggests that its subclonal evolution in and of itself does not

217 cause chemotherapy resistance. Rather, its activation in combination with specific other pathogenic
218 events as part of distinct clones, such as those with mutations of *WT1* or *NUP98* rearrangements or
219 others (6, 38), may cause resistance to chemotherapy.

220 In addition to the marked changes in overall clonal architecture associated with induction
221 chemotherapy, we also observed multiple modes of clonal evolution within individual leukemias. In
222 general, induction chemotherapy induced a relative contraction of the AML cell population, as
223 evidenced by the reduction of the apparent variant allele frequencies (VAF) of mutant genes (mean 0.40
224 versus 0.28 for pre- and post-chemotherapy, respectively, Bonferroni adjusted t-test $p = 2.6e-4$). While
225 VAF contraction was common to most mutations, closer examination of individual patients revealed
226 distinct potential modes of clonal evolution (Figure 4). For example, specimen PASFHK exhibited
227 significant expansion of the *WT1*; *PTCH1*; *ZNF785*-mutant clone, and elimination of the *FLT3*; *SERPIN2*-
228 mutant subclones, upon chemotherapy exposure (Figure 4A). This is consistent with the prior reports of
229 elimination of *FLT3*-mutant subclones upon AML relapse (5), supporting the proposal that activated *FLT3*
230 contributes to chemotherapy resistance only when present with specific cooperating mutations, such as
231 *WT1*. For specimen PATJMY, we observed evolution of a new loss-of-function nonsense mutation of
232 *CHMP6*, which emerged either upon chemotherapy exposure or was selected as a pre-existing subclone,
233 present at less than 2% fraction at diagnosis, given the 50-fold sequencing coverage for *CHMP6* (Figure
234 4B). Reduced *CHMP6* gene expression has been associated with inferior survival of elderly AML patients
235 (39), and its function in endosomal cell surface receptor recycling may contribute to chemotherapy
236 resistance (40). In agreement with prior reports (7), specimen PASTZK exhibited subclonal evolution of
237 mutant *TP53* at diagnosis, which led to its clonal expansion in combination with clonal *PHF6* mutation
238 upon chemotherapy administration, in contrast to mutation of *NRAS* which remained subclonal (Figure
239 4C). Finally, specimen PARXYR exhibited relative contraction of the *WT1*; *PTPN11*-mutant subclone, and
240 relative expansion of the *GPR137B*-mutant subclone that additionally acquired a *CD82* mutation (Figure

241 4D). Other leukemias showed similar subclonal composition pre- and post-treatment, such as for
242 specimen PARBT, which demonstrated the likely pathogenic *IDH2* R172K (VAF 0.58 pre and 0.45 post)
243 and *H3F3A* K27M mutations (0.46 pre and 0.54 post). These findings demonstrate distinct modes of
244 clonal selection upon chemotherapy exposure, which are expected to inform future targeting of specific
245 molecular mechanisms to overcome or block chemotherapy resistance.

246

247 **Discussion**

248

249 Our study defines the genomic landscape of pediatric AML with primary chemotherapy
250 resistance and failure of induction remission therapy. Importantly, primary chemotherapy resistant
251 pediatric AML involves multiple distinct genetic mechanisms. Most notably, we found substantial
252 prevalence of structural rearrangements, at least some of which are associated with the expression of
253 chimeric fusion genes. In particular, we observed at least three distinct genetic groups of patients with
254 induction failure, including those with *NUP98* rearrangements, somatic mutations of *WT1*, *ELF1*, *KMT2C*,
255 *MLLT10*, and additional recurrent gene mutations, fusions, and structural rearrangements, some of
256 which have been observed in other malignancies. Given the known technical challenges with the
257 detection of genomic rearrangements and gene fusions (41), it is possible that additional pathogenic
258 structural variants or chimeric gene fusions may contribute to AML and primary chemotherapy
259 resistance.

260 In our prior study of primary chemotherapy resistance, we identified individual mutations of
261 *ASXL1*, *SETBP1* and *RELN* to be significantly enriched in a subset of pediatric AML with primary induction
262 failure (8). Insofar as *ASXL1* and *WT1* mutations are mutually exclusive in both pediatric and adult AML,
263 the prevalence of *WT1* mutations and absence of apparent *ASXL1* mutations in our current cohort
264 suggests that additional genetic mechanisms of primary chemotherapy resistance likely exist. Our results

265 also suggest that varied genetic mechanisms of chemotherapy resistance may converge on coherent
266 gene expression programs, at least insofar as they cannot be statistically decomposed using matrix
267 factorization used as part of this gene set enrichment analysis.

268 Importantly, our study identified distinct combinations of mutations that appear to be
269 associated with primary chemotherapy resistance. In particular, we observed an association between
270 *NUP98-NSD1* fusions and mutations of *WT1*, *ELF1* and *FRMD8*, suggesting possible cooperativity in their
271 pathogenic functions. Similarly, we observed an association between *WT1* mutations and
272 rearrangements of *BCL11B* and *ARID1B* loci, both of which encode components of the SWI/SNF/BAF
273 chromatin remodeling complex. Notably, *BCL11B* is recurrently mutated in refractory forms of T-ALL,
274 which may share common origins with subsets of AML (20). Evidently, these combinatorial mechanisms
275 in pediatric AML are distinguished from other mechanisms of chemotherapy resistance, such as
276 inactivation of *TP53* in adult AML (7).

277 Our study identified additional mutations associated with pediatric primary chemotherapy
278 resistance. This includes loss-of-function mutations of *KMT2C*, which encodes a component of the MLL3
279 chromatin remodeling complex, potentially similar to the deletions of chromosome 7q observed in high-
280 risk AML that involve this locus and have been found to confer susceptibility to epigenetic therapies
281 (23). We also observed deletions of *MLLT10*, which is recurrently rearranged as gene fusions in subsets
282 of T-ALL. Insofar as *MLLT10* is a cofactor of the DOT1L methyltransferase, this may be associated with
283 the susceptibility to emerging DOT1L methyltransferase inhibitors such as pinometostat (EPZ-5686),
284 which will need to be tested in future studies. Additional mutations associated with primary
285 chemotherapy resistance may be found in larger studies. For instance, the presence of likely pathogenic
286 *IDH2* R172K and *H3K27M* K27M mutations in one specimen in our cohort suggests additional potential
287 mechanisms of chemotherapy resistance (42-45), which may confer susceptibility to emerging therapies
288 such as the IDH inhibitor enasidenib (AG-221) for example.

289 Our findings also suggest that the diversity of genetic chemotherapy resistance mechanisms
290 may be associated with variable outcomes of intense combination chemotherapy in AML. Importantly,
291 increase in the apparent prevalence and allelic frequency of genetic clones with mutations of *FRMD8*,
292 *FANK1*, *PIK3R1*, *WT1* and others indicate that these alleles, in cooperation with *NUP98-NSD1* and other
293 initiating mutations, may directly cause chemotherapy resistance. In contrast, subclonal mutations of
294 *FLT3*, *PTPN11* and *NRAS* were reduced or eliminated by chemotherapy, suggesting that these secondary
295 mutations in and of themselves do not cause chemoresistance. Indeed, subclonal mutations of *FLT3* or
296 *NRAS* were not significantly associated with primary chemotherapy resistance in our prior study (8).
297 Diverse genetic mechanisms of chemotherapy resistance may be associated with clonal evolution (5, 6),
298 as also evidenced by our findings (Figures 3 and 4). On the other hand, common gene expression
299 programs may be associated with shared molecular dependencies, substantiating the development of
300 targeted therapies, as recently evidenced by molecular therapy of MEF2C in chemotherapy resistant
301 AML (46).

302 In all, our study demonstrates that primary chemotherapy resistance and failure of induction
303 chemotherapy in pediatric AML is associated with multiple genetic mechanisms, and exhibits diverse
304 clonal dynamics, dependent on distinct combinations of mutations. Future functional studies will be
305 needed to assess the mechanisms of cooperativity among the observed chemotherapy-associated
306 mutations and their specific pharmacologic targeting. Similarly, additional studies will be needed to
307 define the prognostic significance of the observed chemotherapy-associated mutations. This is expected
308 to delineate molecular mechanisms of primary chemotherapy resistance in pediatric AML, which should
309 inform improved approaches for its diagnosis and therapy.

310

311

312

313

314 **Acknowledgements.** This paper is dedicated to the memory of Dr. Robert Arceci. This work was
315 supported by the NCI U10 CA98543 (TARGET), U24 CA114766 (COG), U10 CA180886, U10 CA098413,
316 U10 CA180899, P30 CA008748, R01 CA204396, by the Damon Runyon-Richard Lumsden Foundation
317 Clinical Investigator and St. Baldrick's Foundation Arceci Innovation Awards (A.K.), and the Charles E.
318 Trobman Scholarship (N.M.). We thank T. Davidsen and P. Gesuwan for their support of the TARGET
319 Data Coordinating Center, and Alejandro Gutierrez, Gila Spitzer, and Maria Luisa Sulis for comments on
320 the manuscript.

321

322 **References**

- 323 1. Rasche M, Zimmermann M, Borschel L, Bourquin JP, Dworzak M, Klingebiel T, et al. Successes
324 and challenges in the treatment of pediatric acute myeloid leukemia: a retrospective analysis of the
325 AML-BFM trials from 1987 to 2012. *Leukemia*. 2018.
- 326 2. Ley TJ, Ding L, Walter MJ, McLellan MD, Lamprecht T, Larson DE, et al. DNMT3A mutations in
327 acute myeloid leukemia. *N Engl J Med*. 2010;363(25):2424-33.
- 328 3. Mardis ER, Ding L, Dooling DJ, Larson DE, McLellan MD, Chen K, et al. Recurring mutations found
329 by sequencing an acute myeloid leukemia genome. *N Engl J Med*. 2009;361(11):1058-66.
- 330 4. Papaemmanuil E, Gerstung M, Bullinger L, Gaidzik VI, Paschka P, Roberts ND, et al. Genomic
331 Classification and Prognosis in Acute Myeloid Leukemia. *N Engl J Med*. 2016;374(23):2209-21.
- 332 5. Ding L, Ley TJ, Larson DE, Miller CA, Koboldt DC, Welch JS, et al. Clonal evolution in relapsed
333 acute myeloid leukaemia revealed by whole-genome sequencing. *Nature*. 2012;481(7382):506-10.
- 334 6. Farrar JE, Schuback HL, Ries RE, Wai D, Hampton OA, Trevino LR, et al. Genomic Profiling of
335 Pediatric Acute Myeloid Leukemia Reveals a Changing Mutational Landscape from Disease Diagnosis to
336 Relapse. *Cancer Res*. 2016;76(8):2197-205.
- 337 7. Klco JM, Miller CA, Griffith M, Petti A, Spencer DH, Ketkar-Kulkarni S, et al. Association Between
338 Mutation Clearance After Induction Therapy and Outcomes in Acute Myeloid Leukemia. *JAMA*.
339 2015;314(8):811-22.
- 340 8. Brown FC, Cifani P, Drill E, He J, Still E, Zhong S, et al. Genomics of primary chemoresistance and
341 remission induction failure in paediatric and adult acute myeloid leukaemia. *Br J Haematol*.
342 2017;176(1):86-91.
- 343 9. Brown FC, Still E, Koche RP, Yim CY, Takao S, Cifani P, et al. MEF2C Phosphorylation Is Required
344 for Chemotherapy Resistance in Acute Myeloid Leukemia. *Cancer Discov*. 2018;8(4):478-97.
- 345 10. Laszlo GS, Alonzo TA, Gudgeon CJ, Harrington KH, Kentsis A, Gerbing RB, et al. High expression of
346 myocyte enhancer factor 2C (MEF2C) is associated with adverse-risk features and poor outcome in
347 pediatric acute myeloid leukemia: a report from the Children's Oncology Group. *J Hematol Oncol*.
348 2015;8:115.
- 349 11. Bolouri H, Farrar JE, Triche T, Jr., Ries RE, Lim EL, Alonzo TA, et al. The molecular landscape of
350 pediatric acute myeloid leukemia reveals recurrent structural alterations and age-specific mutational
351 interactions. *Nat Med*. 2018;24(1):103-12.
- 352 12. Gamis AS, Alonzo TA, Meschinchi S, Sung L, Berbing RB, Raimondi SC, et al. Gemtuzumab
353 Ozogamicin in children and adolescents with de novo acute myeloid leukemia improves event-free
354 survival by reducing relapse risk: results from the randomized phase III children's oncology group trial
355 AAML0531. *Journal of Clinical Oncology*. 2014;32(27):3021-3032.
- 356 13. Cancer Genome Atlas Research N, Ley TJ, Miller C, Ding L, Raphael BJ, Mungall AJ, et al. Genomic
357 and epigenomic landscapes of adult de novo acute myeloid leukemia. *N Engl J Med*. 2013;368(22):2059-
358 74.
- 359 14. Hollink IH, van den Heuvel-Eibrink MM, Arentsen-Peters ST, Pratcorona M, Abbas S, Kuipers JE,
360 et al. NUP98/NSD1 characterizes a novel poor prognostic group in acute myeloid leukemia with a
361 distinct HOX gene expression pattern. *Blood*. 2011;118(13):3645-56.

362 15. Ostronoff F, Othus M, Gerbing RB, Loken MR, Raimondi SC, Hirsch BA, et al. NUP98/NSD1 and
363 FLT3/ITD coexpression is more prevalent in younger AML patients and leads to induction failure: a COG
364 and SWOG report. *Blood*. 2014;124(15):2400-7.

365 16. Ando K, Tsushima H, Matsuo E, Horio K, Tominaga-Sato S, Imanishi D, et al. Mutations in the
366 nucleolar phosphoprotein, nucleophosmin, promote the expression of the oncogenic transcription
367 factor MEF/ELF4 in leukemia cells and potentiates transformation. *J Biol Chem*. 2013;288(13):9457-67.

368 17. da Silva-Coelho P, Kroese LI, Yoshida K, Koorenhof-Scheele TN, Knops R, van de Locht LT, et al.
369 Clonal evolution in myelodysplastic syndromes. *Nat Commun*. 2017;8:15099.

370 18. Lavallee VP, Lemieux S, Boucher G, Gendron P, Boivin I, Girard S, et al. Identification of MYC
371 mutations in acute myeloid leukemias with NUP98-NSD1 translocations. *Leukemia*. 2016;30(7):1621-4.

372 19. Miyagi T, Ahuja H, Kubota T, et al. Expression of the Candidate Wilms-Tumor Gene, Wt1, in
373 Human Leukemia-Cells. *Leukemia*. 1993;7(7):970-977.

374 20. Bergmann L, Miethling C, Maurer U, et al. High levels of Wilms' tumor gene (wt1) mRNA in acute
375 myeloid leukemias are associated with a worse long-term outcome. *Blood*. 1997;90(3):1217-1225.

376 21. King-Underwood L, Renshaw J, PritchardJones K. Mutations in the Wilms' tumor gene WT1 in
377 leukemias. *Blood*. 1996;87(6):2171-2179.

378 22. Gutierrez A, Kentsis A, Sanda T, Holmfeldt L, Chen SC, Zhang J, et al. The BCL11B tumor
379 suppressor is mutated across the major molecular subtypes of T-cell acute lymphoblastic leukemia.
380 *Blood*. 2011;118(15):4169-73.

381 23. Chen C, Liu Y, Rappaport AR, Kitzing T, Schultz N, Zhao Z, et al. MLL3 is a haploinsufficient 7q
382 tumor suppressor in acute myeloid leukemia. *Cancer Cell*. 2014;25(5):652-65.

383 24. Gutierrez A, Kentsis A. Acute myeloid/T-lymphoblastic leukaemia (AMTL): a distinct category of
384 acute leukaemias with common pathogenesis in need of improved therapy. *Br J Haematol*.
385 2018;180(6):919-24.

386 25. Brandimarte L, Pierini V, Di Giacomo D, Borga C, Nozza F, Gorello P, et al. New MLLT10 gene
387 recombinations in pediatric T-acute lymphoblastic leukemia. *Blood*. 2013;121(25):5064-7.

388 26. Volinia S, Calin GA, Liu CG, Ambs S, Cimmino A, Petrocca F, et al. A microRNA expression
389 signature of human solid tumors defines cancer gene targets. *Proc Natl Acad Sci U S A*.
390 2006;103(7):2257-61.

391 27. Ovcharenko D, Stolzel F, Poitz D, Fierro F, Schaich M, Neubauer A, et al. miR-10a overexpression
392 is associated with NPM1 mutations and MDM4 downregulation in intermediate-risk acute myeloid
393 leukemia. *Exp Hematol*. 2011;39(10):1030-42 e7.

394 28. Huang JW, Wang Y, Dhillon KK, Calses P, Villegas E, Mitchell PS, et al. Systematic screen
395 identifies miRNAs that target RAD51 and RAD51D to enhance chemosensitivity. *Mol Cancer Res*.
396 2013;11(12):1564-73.

397 29. Liu X, Liao W, Peng H, Luo X, Luo Z, Jiang H, et al. miR-181a promotes G1/S transition and cell
398 proliferation in pediatric acute myeloid leukemia by targeting ATM. *J Cancer Res Clin Oncol*.
399 2016;142(1):77-87.

400 30. Gabra MM, Salmena L. microRNAs and Acute Myeloid Leukemia Chemoresistance: A
401 Mechanistic Overview. *Front Oncol.* 2017;7:255.

402 31. Kunzel U, Grieve AG, Meng Y, Sieber B, Cowley SA, Freeman M. FRMD8 promotes inflammatory
403 and growth factor signalling by stabilising the iRhom/ADAM17 sheddase complex. *Elife.* 2018;7.

404 32. Kategaya LS, Changkakoty B, Biechele T, Conrad WH, Kaykas A, Dasgupta R, et al. Bili inhibits
405 Wnt/beta-catenin signaling by regulating the recruitment of axin to LRP6. *PLoS One.* 2009;4(7):e6129.

406 33. Bou Samra E, Klein B, Commes T, Moreaux J. Development of gene expression-based risk score
407 in cytogenetically normal acute myeloid leukemia patients. *Oncotarget.* 2012;3(8):824-32.

408 34. Abu-Duhier FM, Goodeve AC, Wilson GA, Gari MA, Peake IR, Rees DC, et al. FLT3 internal
409 tandem duplication mutations in adult acute myeloid leukaemia define a high-risk group. *Br J Haematol.*
410 2000;111(1):190-5.

411 35. Meshinchi S, Woods WG, Stirewalt DL, Sweetser DA, Buckley JD, Tjoa TK, et al. Prevalence and
412 prognostic significance of Flt3 internal tandem duplication in pediatric acute myeloid leukemia. *Blood.*
413 2001;97(1):89-94.

414 36. Thiede C, Steudel C, Mohr B, Schaich M, Schakel U, Platzbecker U, et al. Analysis of FLT3-
415 activating mutations in 979 patients with acute myelogenous leukemia: association with FAB subtypes
416 and identification of subgroups with poor prognosis. *Blood.* 2002;99(12):4326-35.

417 37. Schlenk RF, Kayser S, Bullinger L, Kobbe G, Casper J, Ringhoffer M, et al. Differential impact of
418 allelic ratio and insertion site in FLT3-ITD-positive AML with respect to allogeneic transplantation. *Blood.*
419 2014;124(23):3441-9.

420 38. Garg M, Nagata Y, Kanojia D, Mayakonda A, Yoshida K, Haridas Keloth S, et al. Profiling of
421 somatic mutations in acute myeloid leukemia with FLT3-ITD at diagnosis and relapse. *Blood.*
422 2015;126(22):2491-501.

423 39. Visani G, Ferrara F, Di Raimondo F, Loscocco F, Fuligni F, Paolini S, et al. Low-dose lenalidomide
424 plus cytarabine in very elderly, unfit acute myeloid leukemia patients: Final result of a phase II study.
425 *Leuk Res.* 2017;62:77-83.

426 40. Yorikawa C, Shibata H, Waguri S, Hatta K, Horii M, Katoh K, et al. Human CHMP6, a myristoylated
427 ESCRT-III protein, interacts directly with an ESCRT-II component EAP20 and regulates endosomal cargo
428 sorting. *Biochem J.* 2005;387(Pt 1):17-26.

429 41. Kumar S, Vo AD, Qin F, Li H. Comparative assessment of methods for the fusion transcripts
430 detection from RNA-Seq data. *Sci Rep.* 2016;6:21597.

431 42. Wang F, Travins J, Delabarre B, Penard-Lacronique V, Schalm S, et al. Targeted inhibition of
432 mutant IDH2 in leukemia cells induces cellular differentiation. *Science.* 2013;340(6132):622-6.

433 43. Lewis PW, Muller M, Koletsky MS, Cordero F, Lin S, et al. Inhibition of PRC2 activity by gain-of-
434 function H3 mutation found in pediatric glioblastoma. *Science.* 2013;340(6134):857-61.

435 44. Lehnertz B, Zhang Y, Boivin I, Mayotte N, Tomellini E, et al. H3K27M mutations promote context-
436 dependent transformation in acute myeloid leukemia with *RUNX1* alterations. *Blood.*
437 2017;130(20):2204-14.

438

439 45. Kernytsky A, Wang F, Hansen E, Schalm S, Straley K, et al. IDH2 mutation-induced histone and
440 DNA hypermethylation is progressively reversed by small-molecule inhibition. *Blood*. 2015;125(2):296-
441 303.

442 46. Vakoc CR, Kentsis A. Disabling an oncogenic transcription factor by targeting of control kinases.
443 *Oncotarget*. 2018;9(64):32276-7.

444

445

446

447

448

449

450

451

452

453

454

455

456

457

458

459

460

461

462

463

464

465

466

467

468

469

470

471 **FIGURE LEGENDS**

472

473 **Figure 1: Recurrently mutated genes in pediatric induction failure AML identified by whole-genome**
474 **and RNA sequencing analysis. (a)** Top 20 most commonly called mutated genes, with the mutation type
475 indicated by color, observed at diagnosis, enumerated by the number of total calls, independent of
476 patient assignment. **(b)** Circos plot of high-confidence gene fusions, identified from combined analysis of
477 RNA and whole-genome sequencing data, observed at diagnosis. All variants are tabulated as fusions for
478 calls from RNA-seq, structural variants when called from whole-genome sequencing, and both when
479 both the fusion and supporting genomic structural variants match.

480

481 **Figure 2: Three groups of pediatric induction failure AML identified by whole-genome and RNA**
482 **sequencing analysis. (a)** Tile plot of recurrently mutated genes and gene expression profiles by patient,
483 showing three disease groups, as labeled, with each row listing the mutant gene, and each column
484 representing an individual patient specimen: Group 1, defined by *NUP98* alterations (patients with
485 *NUP98-NSD1* fusions except patient 1 with *NUP98* gain); Group 2, defined by *WT1* mutations, and Group
486 3, defined by the apparent absence of *NUP98* or *WT1* mutations. **(b)** Gene set enrichment analysis
487 (GSEA) of the three patient groups, listing significantly enriched (red) and downregulated (blue) gene
488 sets, as a function of their normalized enrichment.

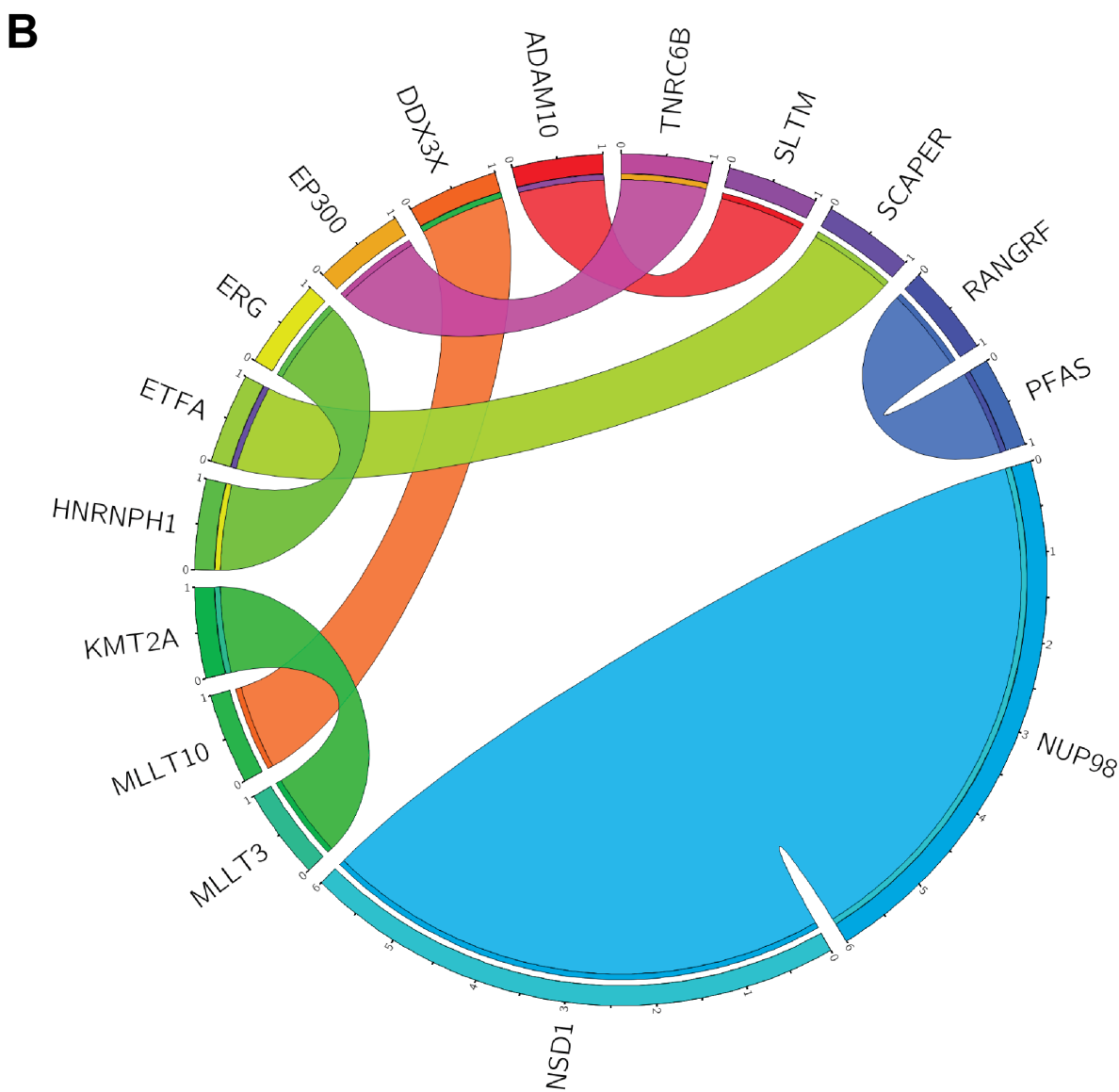
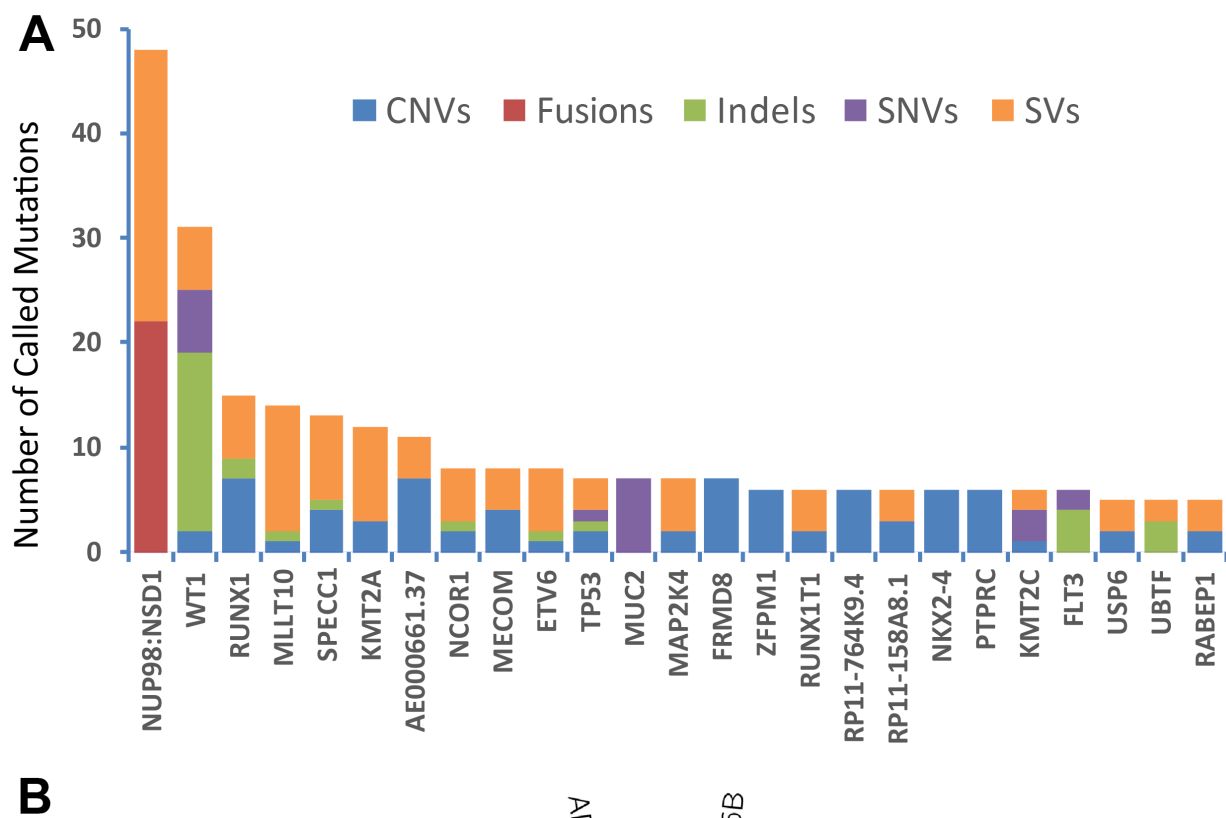
489

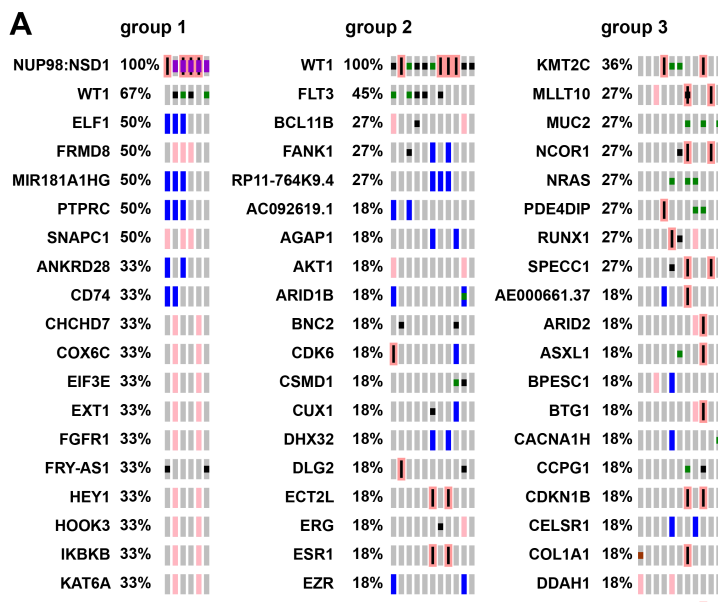
490 **Figure 3: Clonal selection upon chemotherapy treatment.** Tile plot showing recurrently mutated genes
491 with changes in apparent allele frequencies upon induction chemotherapy. For *FLT3* mutations, TKD
492 mutations are listed as SNVs, and ITDs as indel mutations.

493

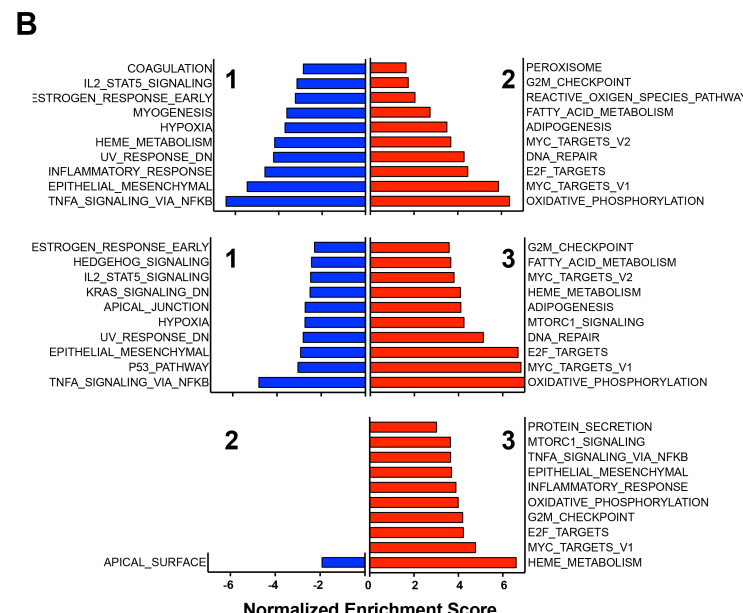
494 **Figure 4: Mutant allele frequencies suggest diverse modes of clonal evolution upon chemotherapy**
495 **exposure.** Variant allele frequencies (VAF) in four specimens with *WT1* mutant clones are represented
496 as the height of color-coded clones, with full height of allele frequency axis corresponding to a mutant
497 allele frequency of 1. Simplest models of clonal architecture are shown, with additional models possible.
498 Each hypothesized subclone is represented by a different color. **(a)** Specimen PASFHK in Group 2, largest
499 VAF at diagnosis was 0.96 for *WT1* R430P; largest VAF at induction failure was 0.38 for *WT1* R430P. **(b)**
500 Specimen PATJMY in Group 1, largest VAF at diagnosis was 0.53 for *WT1* S381, largest VAF at induction
501 failure was 0.47 for *CHMP6* E108stop. **(c)** Specimen PASTZK in Group 2, largest VAF at diagnosis was 0.77
502 for *PHF6* R370stop, largest VAF at induction failure was 0.37 for *TP53* R273C. **(d)** Specimen PARXYR in
503 Group 1, largest VAF at diagnosis was 0.57 for *RBAK* V708I, largest VAF at induction failure was 0.43 for
GPR137B T182M.

504



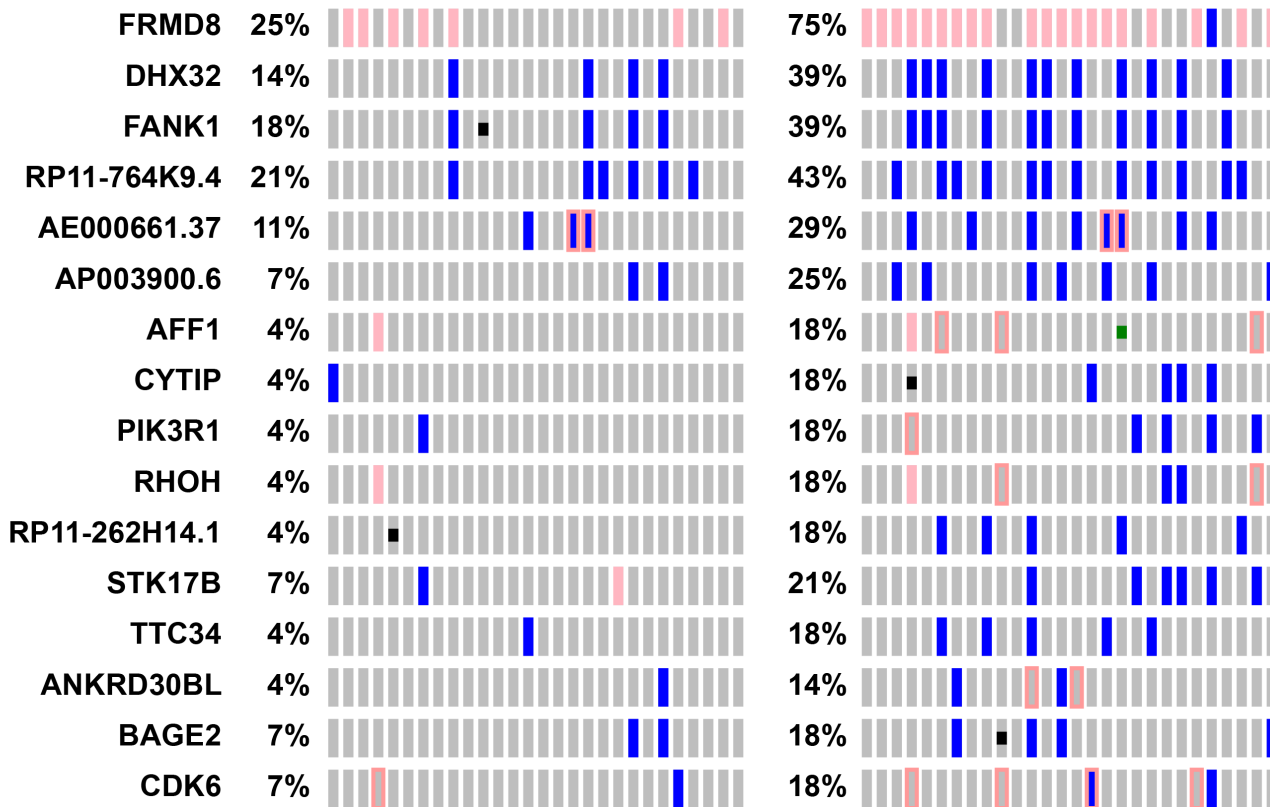


No alterations Gain Deep Deletion Structural Variant Fusion SNV Indel

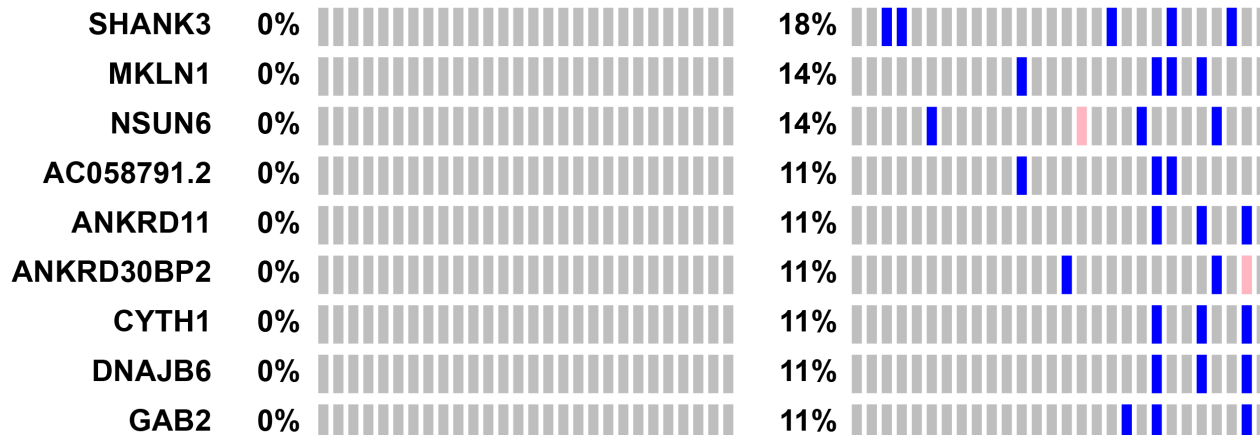


Pre-Treatment Post-Treatment

increased in post treatment



present in only post treatment



decreased in post treatment



No alterations Gain Deep Deletion Structural Variant Fusion
 SNV Indel

